AN EXPERIMENTAL INVESTIGATION ON WING BOX BEAMS IN BENDING

by

E. Antona, Professore Incaricato
and
G. Gabrielli, Professore Ordinario
Politecnico di Torino, Italy

The Seventh Congress of the International Council of the Aeronautical Sciences

AN EXPERIMENTAL INVESTIGATION ON WING BOX BEAMS IN BENDING

E.ANTONA and G.GABRIELLI
Istituto di Progetto di Aeromobili
Politecnico di Torino

Abstract

The behaviour of typical wing box beams in bending at increasing load levels up to failure is investigated by testing a set of specimens formed by two spars, two longitudinally stiffened flat panels and a few intermediate bulkheads varying in number from one to three. The panels are of two types, one with riveted extruded ⌐-stiffeners, and another with integral stiffeners.

The effects of crushing pressure, bulkhead flexural deformations and structure initial imperfections are particularly emphasized.

The experimental results indicate that such effects are remarkable for the structures under investigation.

They cover deformation components which, with increasing load levels, induce local failure stresses in addition to instability phenomena.

Introduction

The main strength components of a shell structure in modern aircraft mainly consist of flat or curved panels generally stiffened and other typical elements, such as frames, bulkheads and spars. In particular, today's wings are made up of structures consisting of flat or flat-like panels, spars and bulkheads. As to panels, they may be of the composite, integral or sandwich types.

Presently many experimental and basic research results are available on flat panels. However, they mostly examine the features of panel buckling and failure loads under various load conditions and different constraints at edges, but the panels themselves are considered as isolated and detached from their main structure. Obviously, the results so obtained cannot simply be applied to the same panels when they are an integral part with structure. And this mainly for the reasons that the actual conditions at edges and deformations, induced into the panel within the wing structure, considerably affect panel behaviour and originate problems not be evidenced when testing the isolated panel.

As regards boundary conditions along panel edges, researches on isolated panels usually assume them as actually known (and expressible, for example, as constraints coefficients), so that, when testing isolated panels where various boundary conditions are realized, one could foresee the actual behaviour of the panel in the structure.

However, actual boundary conditions of panel within the structure are far from being known. Therefore, the only manner to obtain results directly usable in calculations is to include the same constraints in the body under study.

Deformations, induced into the panel by its parent structure in actual operation, play an important role, mainly for the effects of crushing pressure and anticlastic curvature. It is well known that crushing pressure in wing box [6] originates from the simultaneous presence of longitudinal stresses and local values of length-wise curvature, the latter being caused by box curvature and local values of curvatures due to panel deformations versus configuration as foreseen in the linear theory, [6] and [9].

Anticlastic curvature due to the effect of transverse contraction is always associated to bulkhead flexural deformability and induces effects involving box behaviour, specially when bulkheads show deformability degrees different from each other. Furtherly, the influence of initial imperfections against nominal dimensions should also be considered. Obviously, such influence also appears on isolated panels.

o o o

It is known that, under given load conditions, structural elements exhibit failures due to equilibrium instability phenomena in addition to failures connected with critical local stresses. Such phenomena appear as deformations through which the element tries to avoid loads. They are distinguished in global and local instability phenomena according to whether, in determining their inception conditions there intervene the major dimensions and boundary conditions of the panel itself or not. For example, instability phenomena involving both length and width of the panel, are called global phenomena. Local phenomena, on the other hand, are the ones which are not affected either by length or width of the panel. Obviously, also a transition region is to be considered.

The mechanism leading to breakage, however, may be very complicated because in a complex structure the appearance of a phenomenon on a local scale will not necessarily end in a failure. For example, flat stiffened panels may exhibit initial buckles (either on skin or stiffeners) affecting strain distribution at a further load increase and generally reducing strength, but still leaving residual strength capabilities to the structure. A load increase may result either in a failure due to local instability (when the other component – stiffener or skin – collapses locally) or a failure due to global instability. Deformations connected with a change of structure shape, though important from a theoretical standpoint, have no practical bearing on the structures commonly used in wing strength components. As a matter of fact, such effects appear when deforma-

tions are rather large and involve non-linear de-
flections.

Instead,some components where initial buckling
has occurred often show a decreased capability of
withstanding further deformation.

When dealing with stability problems through diffe-
rential equations of equilibrium,in linearized and
homogeneous formulations (i.e.,with known terms
being null) and then valid for small deflections,
instability phenomena clearly appear as indifferent
equilibrium configurations,each one being associa-
ted to a (critical) value of load level.Obviously,
the lower of such critical loads is of practical
interest. Let us see now,from a qualitative view-
point,the effects resulting from the introduction
in the equation of equilibrium of higher order
terms and known terms.

Higher order terms exclude the existence of in-
different equilibrium forms. In addition to the
obvious solution with identically null deforma-
tions, there exist other equilibrium configurations
that, for very small deformations,show a behaviour
asymptotical to the case of indifferent equilibrium
forms. Therefore, the small deformation theory per-
mits to locate values where such equilibrium confi-
gurations originate. Staring from a critical load,
the introduction of non-null deformations in an
equilibrium configuration may be yoined with a load
cecrease. This results is the so called "snap"
collapse (typical, for example, of curvature di-
splaying shells),that practically occurs at load
values than critical load. In case of load increa-
ses, critical load is reached in actual behaviour.
Then large deformations appear for small load incre-
ses,in consequence of a behaviour asymptotical to
the case of indifferent equilibrium forms.

The introduction of known terms excludes the
equilibrium solution with identically null deforma-
tions. However, equilibrium states at increasing
loads are asymptotical, for large deformations, to
equilibrium states where no known terms appear,[9]
and [11]. Crushing pressure, flexural deformation
of bulkheads and initial shape imperfections,par-
ticularly examined in this study,from a mathematical
viewpoint present contributions to known terms and
thus can be introduced into analysis.

Deformations connected with global instability
phenomena (following linearized or more general
formulations) will lead to local stresses causing
failure when the same stresses are increased.Such
a failure can take place by shifting in tensioned
areas, or also in connection with local instability
phenomena in compressed areas. These local instabi-
lities should be theoretically distinguished from
the ones likely to occur separately from deforma-
tions due to global instability and then in absence
of the stresses introduced by the latter.

It is also obvious that, due to the presence of
known terms in the equilibrium equations, an identi
cal (local) deformation is reached for load values
gradually decreasing when known terms are increased.
To this regard,if failure appears when local criti-
cal stresses have been reached, the presence of

known terms may influence breaking load.

Description of tests

The research was carried out on specimens consi-
sting of straight wing box stumps with constant
section, subject to pure bending moment. As regards
the compressed pane,deformations at various load
levels up to failure were examined.

Specimens having the same length, width and height
measured between panel barycentric surfaces differ
from each other for the following features. Panel
structure may be integral or composite. Integral
panels have a cross section area of $843,08$ mm^2 and
composite panels have a cross section area of
$1003,80$ mm^2. Intermediate bulkheads may be 1,2 or
3 in number. Altogether there were 6 types of spe-
cimens, and two samples for each of them.

Specimens being tested are symbolized by a letter
showing panel type (I = integral , C = composite),
followed by bulkhead number (1, 2 or 3) and a letter
(a or b) to distinguish two nominally identical
specimens Fig.1. Nominal dimensions of specimens are
reported in Figs.2 and 3, while deviations of the
various specimens from them are reported in Table I.
Bending machine used in testing (Fig.4) consists of
a frame A, two spar clamps B linked through bolts
C to swinging linkrods D, and two hydraulic jacks
F. Deformations under load of compressed panels
were examined through a centesimal dial indicator
turning on a surface plate and measuring displace-
ments at points of a grid previously traced on the
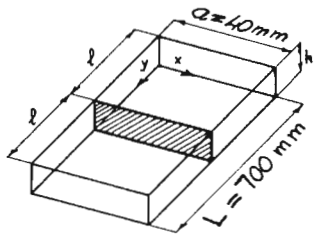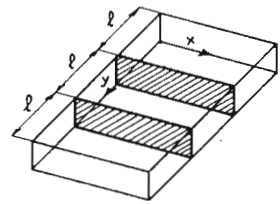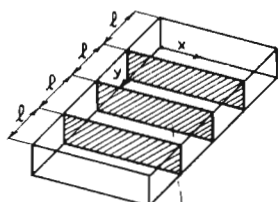panel. In non-destructive tests, longitudinal stress

FIG.1 - Tested specimens

2

were measured at some points of the panel by means of electric strain gages. Also, rotations of clamps were measured through a system of telescopes, mirrors and leveling rods. Tests at increasing loads were performed on each specimen. After every non-destructive test, specimen were unloaded and residual deformations were read.

On integral panel specimens outer strain gauges were placed at the stiffener axes and inner strain gauge pairs were placed at the stiffener centerlines on both ends of the same stiffener (Fig.2). In this case, valid stress values mid-half of stiffeners were obtained by averaging the values of strain gage pairs. In specimen of the composite panel type, the strain gages were placed outside on the skin and inside at the centerline of the $\rfloor$– stiffener flange (Fig.3).

In order to directly utilize generalized results (which by means of the structural similarity law can be extended for every element to a simple infinity structurally similar to it [7]), it is common practice to resort in the representation of results, to the structural load index, which is an invariant in the similarity and contains design data only. In the present case, one can use as structural load index the ratio of the longitudinal stress flux q , acting within panels, and the distance between bulkhead centers [7], the structural load index being M/ahl , where M is the bending moment applied to wing box, a is the width measured between spars (excluding web thickness) and h is the height measured between panel barycentric surfaces (cross sections). The nominal values a = 400 mm and h = 156 mm were adopted, while the values of l 350 mm, 233.3 mm and 175 mm, for 1,2 and 3 intermediate bulkheads, respectively.

R e s u l t s

In all the tests being carried out, the panel longitudinal edges, bound to spar webs, of panels either in compression or in tension, arranged themselves in a form of circle arcs as provided for in the linear theory. By indicating, for every cross section, with f_1 and f_2 cambers at spars, it is worth noting the cambers f of the various points of a panel, minus the average value f_1 and f_2 of the same cross section
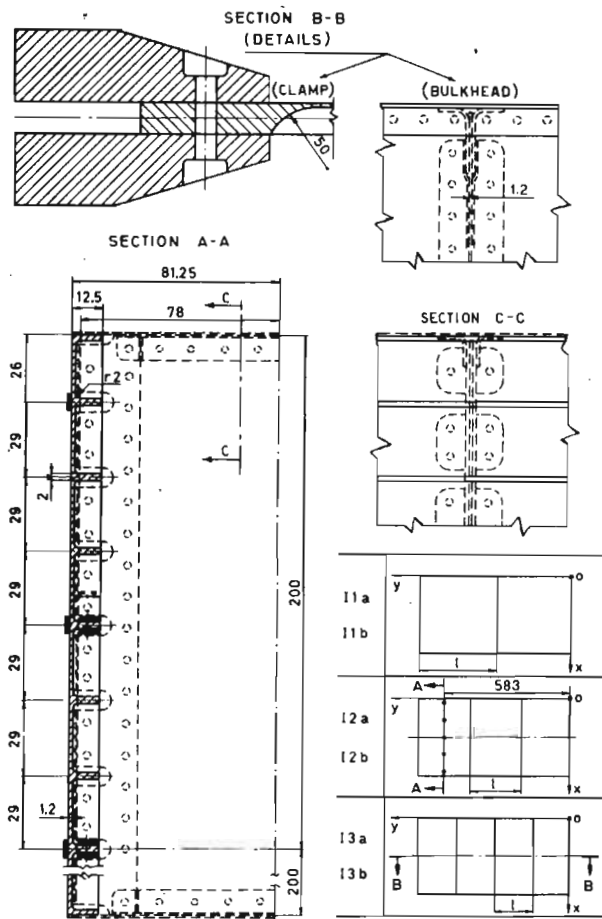

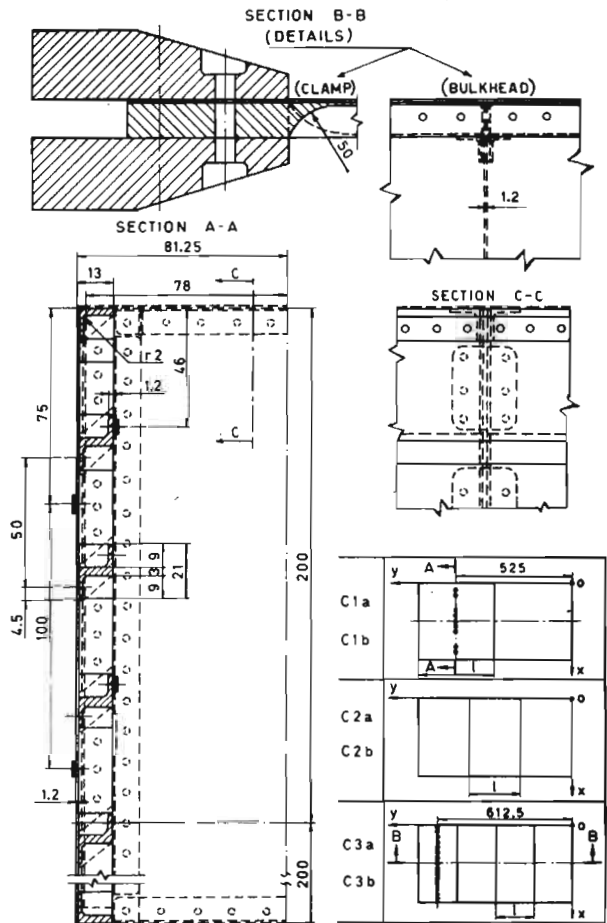FIG.2 – Nominal dimensions of specimens with integrally stiffened panels.

FIG.3 – Nominal dimensions of specimens with stiffened panels.

3

$$w = f - \frac{f_1 + f_2}{2}$$

All the obtained experimental results show values of f_1 and f_2 of the same cross section practically coincident. See also Figs. 5, 6, 7, 8, 9, 10 e 11.

In specimens with integral panels and one bulkhead also at lower load levels, the panel shows a slight asymmetry against the centerline bulkhead, with increased cambers on either spars. This phenomenon is emphasized with increasing loads, thus determining a deformation apparently affected by the presence of initial imperfections. At higher load levels, in approaching a critical value for global elastic instability, there will be a quick evolution towards an antisymmetric trend of the deflection against the centerline bulkhead. On both spans, one buckled inwards and the other outwards, one can observe cambers measured against spars, which are of the same magnitude order (Fig. 6). Breakage will appear in the span deflecting

inward and showing no local instability phenomena, either on stiffeners or on skin. Therefore, because of the global instability, tension stresses in that area are so high as to as to cause failure.

In specimens with integral panels and two bulkheads also at load levels, the compressed panel exibits symmetry both versus longitudinal and transverse centerlines. There are no big local bucklings, and from lower loads levels, an outward bulging appears in the intermediate span. At increasing loads such a bulging shows a non-linear trend of w's, and also an increasing slope at increased values of structural load index (Fig.15). Failure takes place in the intermediate span, which exibits outward shifts. The stiffeners, inside the specimen, whose compression at inner edge is henhanced in the middle of the span by the deformation decribed earlier, exhibit local instability phenomena. Fig.15 shows that deformations are not asymptotical to the value of breaking load, as the evolution of w's in terms of M_f/ahl is interrupted by the intervening failure. In this case, one can

Specimen	Station y [mm]	Skin Average Thickness [mm]	Stiffener Average Thickness [mm]
I 1 a	60	1.20	2.12
	220	1.20	2.15
	·450	1.21	2.15
	680	1.28	2.11
I 1 b	60	1.20	2.09
	240	1.25	2.11
	400	1.28	2.31
	640	1.30	2.35
I 2 a	116	1.283	2.088
	350	1.255	—
	697	1.244	2.123
I 2 b	27	1.276	2.131
	343	1.225	—
	672	1.208	2.064
I 3 b	35	1.279	2.115
	265	1.228	—
	425	1.123	—
	693	1.233	2.135
I 3 b	45	1.262	2.050
	245	1.200	—
	453	1.207	—
	663	1.198	2.108
NOMINAL VALUES		1.20	2.00

a) Integral panel specimens.

Specimen number	Station y [mm]	Skin Average Thickness [mm]	Stiffener Web Average Thickness [mm]
C 1 a	155	1.300	3.007
	330	1.300	3.064
	500	1.312	3.064
	675	1.312	3.074
C 1 b	110	1.187	3.043
	340	1.190	3.043
	498	1.185	3.078
	695	1.185	3.071
C 2 a	135	1.327	3.114
	410	1.327	—
	690	1.322	3.086
C 2 b	130	1.197	3.021
	410	1.195	—
	644	1.187	3.050
C 3 a	152	1.300	3.014
	322	1.312	—
	492	1.310	—
	688	1.312	3.057
C 3 b	70	1.20	3.00
NOMINAL VALUES		1.20	3,00

b) $\rfloor$ - stiffened panel specimens.

TAB. I - Average thickness values measured on the test specimens.

4

deduce that the higher compression stressing acting on stiffeners, directly affect failure because of local instability on stiffeners themselves.

In specimens with integral panels and three bulkheads, deflection trend of w's is symmetrical versus panel centerline and shows no remarkable bulging (Fig.8). Failure occurs at the intermediate span that is deflected inward. It seems to be preceded by the appearance of global instability buckles and occurs through shifting of stiffeners that probably attain critical tension stresses due to the above buckles. Figure 16 seems to confirm such a conclusion, while from strain gauge records no divergence is to be seen (yet) in the difference between stresses and edges (Fig.17 a).

In composite panel specimen, a phenomenon already noted [4] but certainly deserving a further analysis, was observed. It deals with a particular buckling form due to the stiffener considered as isolated, where stiffeners alternately deflect inward and outward so that the skin does not behave as an integral part with them. In such a behaviour the skin seems to fulfill a clamping function between
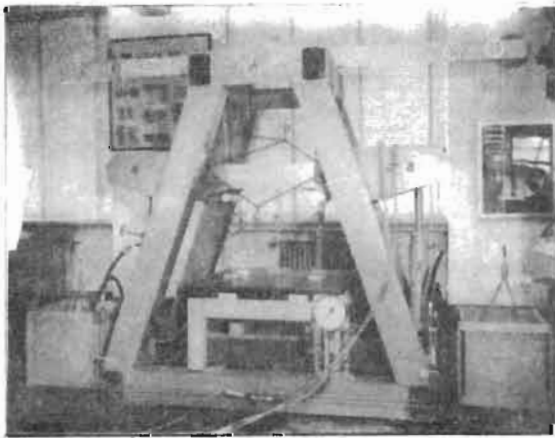

FIG. 4 – Test machine

stiffeners, so that panel maintains remarkable strength capabilities. In the following descriptions, this phenomenon will be referred to as " initial alternate deflection of stiffeners". Deformations due to global instability phenomena, when occurring (specimens C1 and C2), superimpose upon the ones previously recorded and are to be seen even at loads close to breaking loads (Figs. 9 and 10).

Specimen C 1 b initially showed that w's are asymmetrical to longitudinal centerline and bulkhead. Then , starting from areas close to calmps, there appear initial alternate deflections of stiffeners which, at increased loads, extended towards the central area of panel. At the highest loads, panel deflection rapidly evolves towards an antisymmetrical trend of w's typical of global instability, simultaneously enhancing initial phenomena (Fig.9). Breakage occurs in the span deformed inward. Both local instability buckles of some stiffeners near the clamp and stripping of the inner edge at the

span center are recorded. Obviously, the inward deflection of the span enhances compression at the inner (face) near the clamps and tends to generate tension stresses to the same face at the span center. In the evolution of deflection, breaking load seems to be an asymptote to the same deflections. Fig.17 b and w's trends in terms of structural load index (not recorded here for sake of brevity) confirm that breakage is subsequent to local phenomena due to global instability. The specimen C1a showed a failure in the spans deformed outward. Phenomena of local instability were recorded at the inner face of panels, where compresssion stresses were enhanced by deformation due to global instability phenomenon.

In specimens with oomposite panels and two bulkheads, the deflection of compresssed panel is characterized by the presence of initial alternate deflections of stiffeners appearing from lower load levels and clearly spreading, at increased loads, from the areas close to clamps to the areas close to panel centerline (Fig.10). There also appears an evolution of deformations w typical of instability increase. Failure occurs in the intermediate span that deforms outward. Stiffeners, whose compression at outer face is enhanced at the span center, show local instability there. In the spans deformed inward, also residual local buckles appear in the skin. In this specimen, the incidence of local phenomenon on failure must be rather high, when considering that a failure, the global instability had just started.

In specimens with composite panels and three bulkheads, the deflection trend of the compressed panel does not show anything special, except for the appearance, at higher load levels, of initial alternate deflections of stiffeners particularly emphasized near the end areas (Fig.11). In one specimen, breakage occured at the intermediate span (which after failure is deformed outward). In the other specimen, failure occurred near the clamp of a span, which after failure was deformed inward. The trend of w's at increased loads shows that no global instability has occurred. Therefore, we can conclude that it deals with local instability. This is confirmed by the fact that stiffeners, in the failure area, show deformations due to local instability. Also in these specimens, in the spans deformed inward, local buckles on the skin are to be seen.

The main results of the failure tests are summarized in Table II.

Average failure stresses at the panel barycentric surfaces were calculated, according to St.Venant's theory and on the basis of the experimental results, in terms of the structural load indexes of the twelve specimens (Fig.18). On the two particular panels used in the specimens, the integral panel behaves better (i.e., it gives higher average stresses of failure) at the upper values of structural load index. The composite panel, on the other hand, behaves better at the lower values of load structural index.

5

FIG.5 – Specimen I1b tensioned panel.
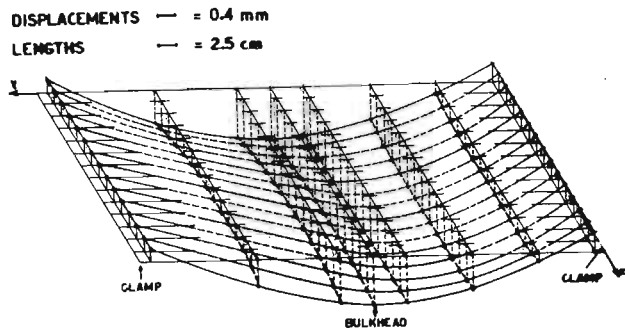Deformed configuration at
$\dfrac{M}{ahl} = 10,68$ kg/cm^2

FIG.6 – Specimen I1b compressed panel.
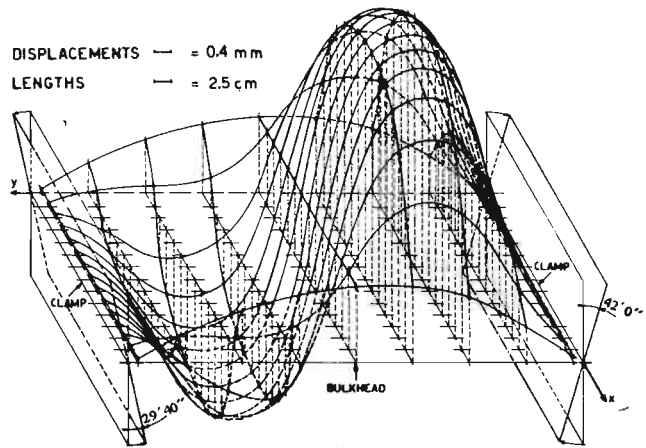Deformed configuration at
$\dfrac{M}{ahl} = 11,8$ kg/cm^2

FIG.7 – Specimen I2a compressed panel.
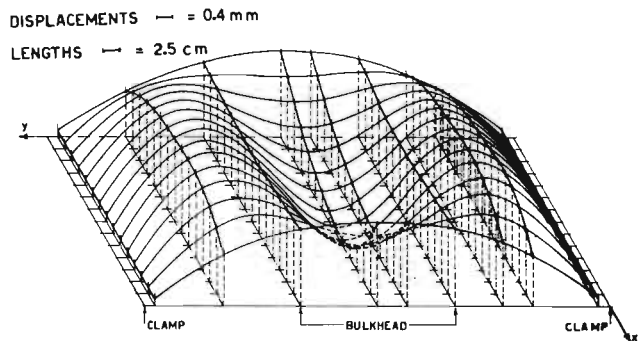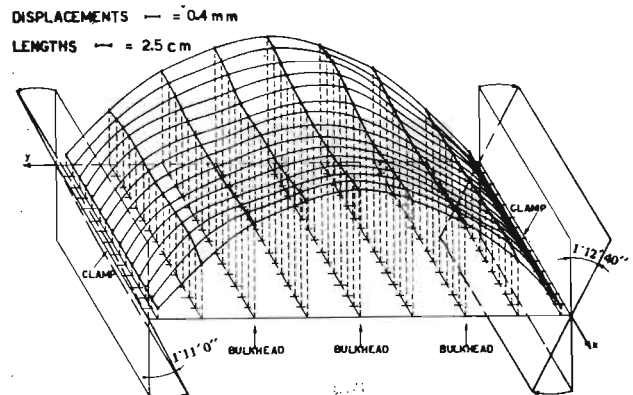Deformed configuration at
$\dfrac{M}{ahl} = 22,7$ kg/cm^2

FIG.8 – Specimen I3b compressed panel.
Deformed configuration at
$\dfrac{M}{ahl} = 47,2$ kg/cm^2

6

In Fig.19 the average stresses resulting from failure tests are reported against the values related to compressed panels of the same section form and material, with free lateral edge, for different values of the constraint coefficient.(*). The

reliability of such values was also confirmed by experimental tests previously performed on isolated panels. In order to evaluate according to Euler its collapsing load, on the basis of a length equal to the distance between bulkheads, the panel free

(*) For the integral panel, global collapse stresses were calculated through Euler formula using tangent module E_t. Local collapse stresses were calculated by resorting to formulas and data as suggested by Shuette [3]. As to composite panels, global collapse stresses were calculated according to the procedure reported by Lundquist [1], who also keeps into account possible initial bucklings

on skin. Local collapse stresses were, however, evaluated according to the procedure indicated by Crockett [2]. The composite panels being considered result both from calculation data free from instability phenomena of skin between rivets and instability phenomena of stiffeners due to unstabilizing action of skin.
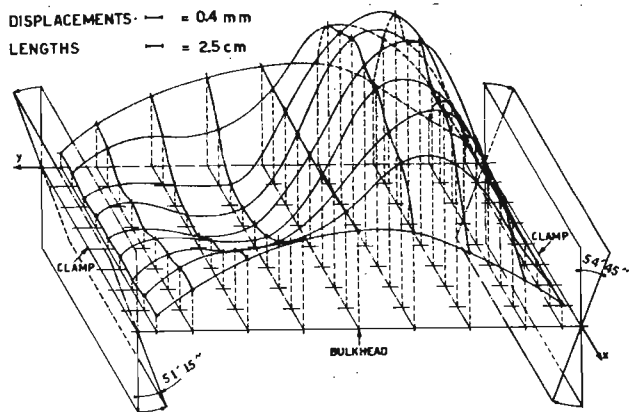

FIG.9 – Specimen C1b compressed panel.
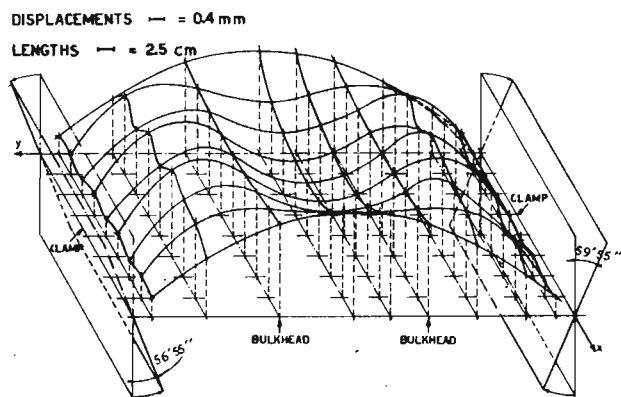Deformed configuration at
$$\frac{M}{ahl} = 18.2 \ kg/cm^2$$

FIG.10 – Specimen C2b compressed panel.
Deformed configuration at
$$\frac{M}{ahl} = 31.1 \ kg/cm^2$$

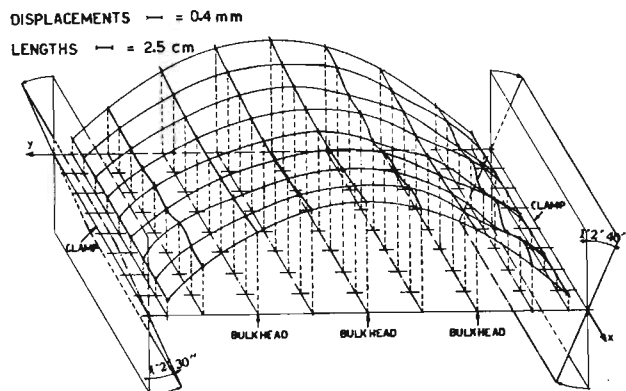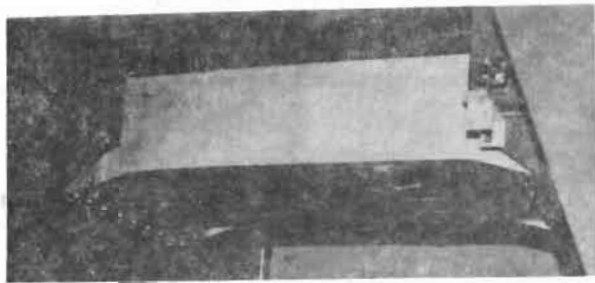FIG.11 – Specimen C3a compressed panel.
Deformed configuration at
$$\frac{M}{ahl} = 46.8 \ kg/cm^2$$

at edges must be assigned with constraint coefficients of $c = 2.04$, $c = 1.50$, $c = 1.30$, for specimens with 1, 2 and 3 intermediate bulkheads, respectively. The comparison with the experimental data on specimens gives interesting indications. As to specimens with integral panels, first it is to be noted that all the results of failure tests have given loads lower than or at maximum equal to the ones of local collapse (derived by calculations). This confirm the deductions previously made on failures for local phenomena due to global instability. In particular, specimens with three bulkheads have given results practically coincident with calculated values of local buckling loads. Such a configuration is therefore practically

– Incipient failure
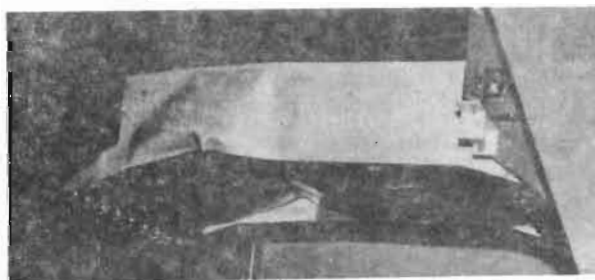
a) Specimen I1b – Failure

a) Specimen C1b – Failure

b) Specimen I2b – Failure

b) Specimen C2a – Failure

c) Specimen I3b – Failure

c) Specimen C3a – Failure

FIG.12 – Failure of integral panel specimens.
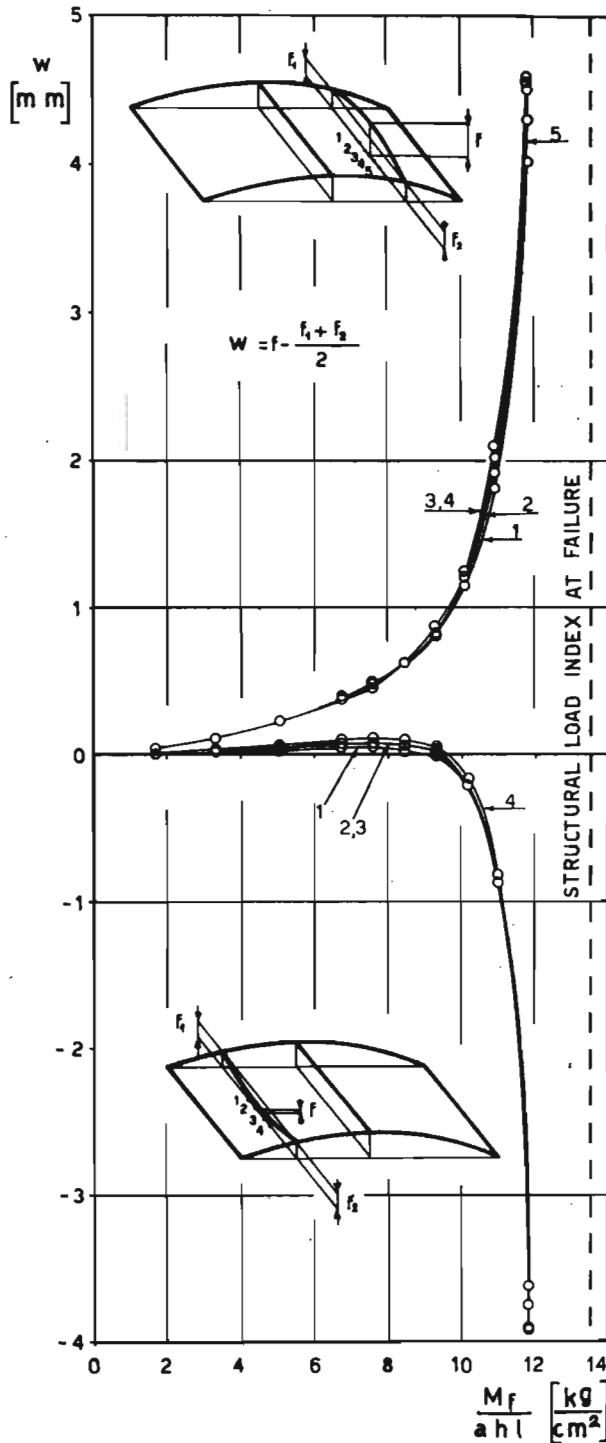
FIG.13 – Failure of composite panel specimens.

8

FIG.14 – Specimen I1b.Deformations in terms of
structural load index.

optimal.

From this standpoint,earlier deductions were also
confirmed for specimens with composite panels.
Among them the panels with one bulkhead undoubtedly
failed because of local phenomena due to global in-
stability. The panels with two bulkheads gave fai-
lure loads practically coincident with local insta-
bility loads (calculated),thus confirming the strong

incidence of local phenomena. The panels with three
bulkheads gave failure loads higher than the cal-
culated ones by keeping into account local insta-
bility. The difference between failure loads of
panels with two and three bulkheads can be explai-
ned when considering the incidence of global phe-
nomena which may precede and enhance local pheno-
mena in two bulkhead specimens.

A comparison (Fig.19) between the values of the
same panels with or without lateral constraints
clearly show the influence of the latter. The ra-
tios of average effective failure stresses and the
comparison stresses in integral panel specimens
are in the order of 1.5 , 1.1and 1.1,with 1,2 and 3

| Speci-men	M $[kgm]$	$\dfrac{M}{ahl}$ $[kg/cm^2]$	Description of failure
I1a	3.085	14.1	1) Global Instability.
I1b	2.940	13.5	2) Stripping of stiffeners in the span which deforms inward due to 1.
I2a	3.675	25.2	1) Global Instability. 2) Local instability of stiffe-ners (intermediate span center)
I2b	3.785	25.9	deformed ouward due to 1.
I3a	5.439	49.8	1) Global Instability. 2) Stripping of stiffeners in
I3b	5.512	50.5	an intermediate span deformed inward due to 1.
C1a	4.480	20.5	1) Initial alternate deflec-tion of stiffeners 2) Global instability 3) Stripping of stiffeners with local buckling of the sa-
C1b	4.336	19.8	me at the clamp in the span that deforms inward or crip-ling of the stringer in the span that deforms outward.
C2a	5.580	38.25	1) Initial alternate deflec-tion of stiffeners. 2) Global instability(initial) 3) Local instability of stif-
C2b	5.218	35.7	feners in an intermediate span deformed outward due to 2.
C3a	6.320	58.0	1) Initial alternate deflec-tion of stiffener. 2) Local instability of stiffe-
C3b	6.064	55.5	ner in the intermediate span or near the clamp.

TAB.II – Results of failure tests.
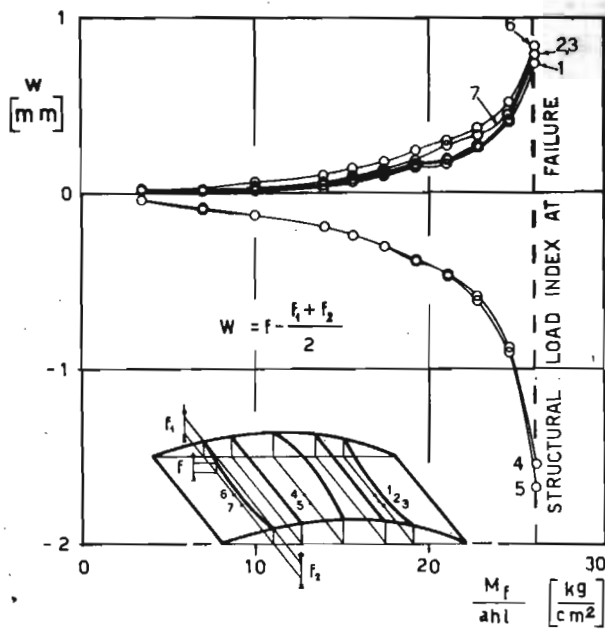
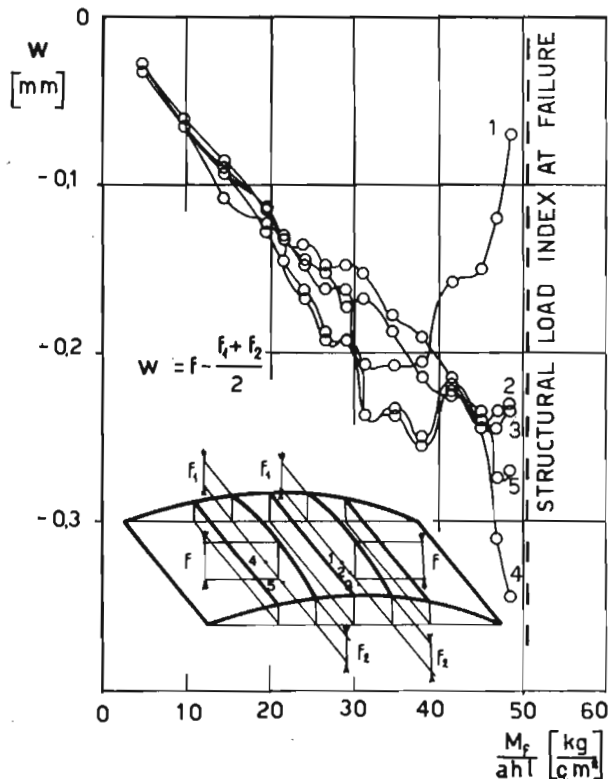FIG.15 – Specimen I2b. Deformations in terms of structural load index.

FIG.16 – Specimen I3b. Deformations in terms of structural load index.

bulkheads, respectively. In specimens with composite panels, excluding the ones with three bulkheads, where failure is due to local phenomena, we have got ratios of about 1.1 and 1 , with 1 and 2 bulkheads respectively. It will be worth noting that such ratios decrease at decreasing length of the span (the width of box beams being equal) and also when failure load gets near the critical load of local instability.

Observations

Anticlastic curvature. The presence of anticlastic curvature, with flexural deformation of bulkheads, will be observed directly from axonometric representation of displacements, in normal direction, of the different points of a panel (see Figs. 6, 7, 8, 9, 10 and 11). The anticlastic curvature is present in all specimens and can be particularly seen in cross sections of panels at bulkheads. To confirm the existence of such curvature, with flexural deformation of bulkheads, there are the results of measurements performed on tensioned panels (Fig.5), which at bulkhead exhibit transverse curvatures of the same sign as the ones of compressed panels.

Crushing pressure. As regards crushing pressure, it appears every time the panel deflection shows evident symmetrical components against the longitudinal and transverse centerlines, not justified by the phenomena of anticlastic curvature. In other words, the effects of crushing pressure are evidentiated by bucklings (having the above symmetries) in the inward direction. E.Antona and P.Pelagalli in a previous work [10], by referring to the specimen Cla, where the effects due to initial imperfections were minor, made a comparison between deflections calculated theoretically by keeping into account crushing pressure and anticlastic curvature, and obtained experimental results related to the longitudinal section of the panel centerline. Such a comparison has indicated that theory is in good agreement with experience. This confirms the presence, in the flexural behaviour of boxed beams, of anticlastic curvature and crushing pressure.

Local buckling. Among the various buckling phenomena, first we willexamine the ones that,having appeared before global phenomena, did not cause structure collapse but only changes to geometrical configuration and stress distribution with which the different specimens, at increasing loads,have proceeded towards collapse. The most significant phenomena to this respect appeared in composite panels as instability phenomena, each stiffener being considered as a column (with intermediate rests on bulkheads). The stiffeners in the single spans between bulkheads alternately buckled inward and outward and exhibited twists in the same spans. In the involved area, the skin showed along cross sections a typical waviness beyond critical load as indicated in Figs.9, 10 and 11. It is manifest that deformations due to such a phenomenon are superimpo-

10
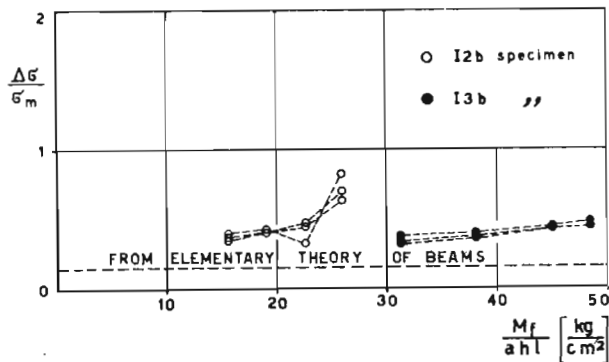
a) Integral panel specimens.
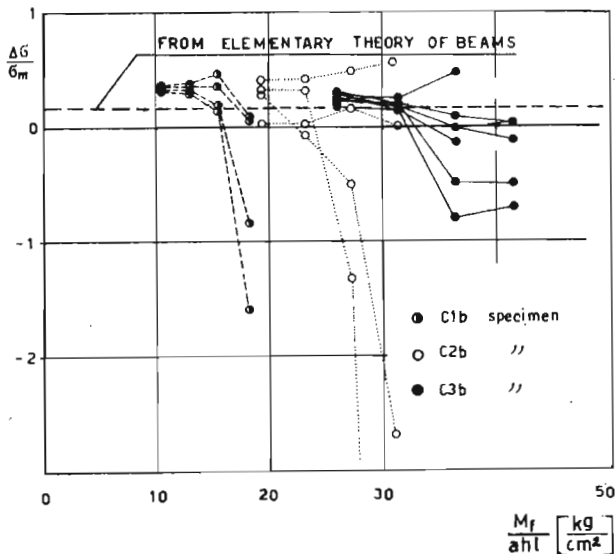
b) Composite panel specimen.

FIG.17 – Trends of $\frac{\Delta\sigma}{\sigma_m}$ in terms of structural load index.

sed upon the ones due to the anticlastic curvature and crushing pressure.

Initial imperfections. The effects of initial imperfection instead are to be seen, for loads lower than critical ones, in all the panel deflections which do not respect symmetries against the longitudinal plane of symmetry and centerline. The above-mentioned comparison between theory and experience [10], where theory validity is verified by the very good correspondence with experience in cases free of initial error effects, has offered the opportunity of evaluating the magnitude order of such effects. In fact, they can be deduced as a difference between the deformations obtained experimentally and the calculated ones, by keeping into account every other effect except for the one

in question. The result [10] in such a case is that said deformations are of the same magnitude order as the ones connected with all remaining causes.

Phenomena of global instability. The majority of specimens exhibited instability. They manifest with the increase, according to ever increasing slope trends, of relevant deformation components when applied loads are increasing. From Figs. 14, 15 and 16, recording displacement trends of some points of panels compressed in terms of structural load index, in some specimens one can note clusters of points with ever steeper displacements as well as clusters of points whose displacements initally show the same sign as for previous ones and finally annul and acquire rapidly increasing values of apposite sign (*). As displacements due to orthogonal pressure and bulkhead deformations must at varied loads (nominally) have constant and uniform sign at all points of the panel, besides enjoying symmetries against longitudinal and transverse centerlines, the trends diverging from this clearly show the prevalence of such effects at lower loads, and also the appearence at higher loads of global instability phenomena that give non–symmetrical displacements.

Strain gage measurements. The results of strain gage measurements underline the emergence of additional stresses, versus the values of linear theory, due to the effects described above. Fig.17 reports the ratios at various load levels, of the spread between stresses at inner and outer surfaces of the compressed panel, and the value σ_m at the panel barycentric surfaces. In view of the tested model geometry, the nominal value of the ratio in
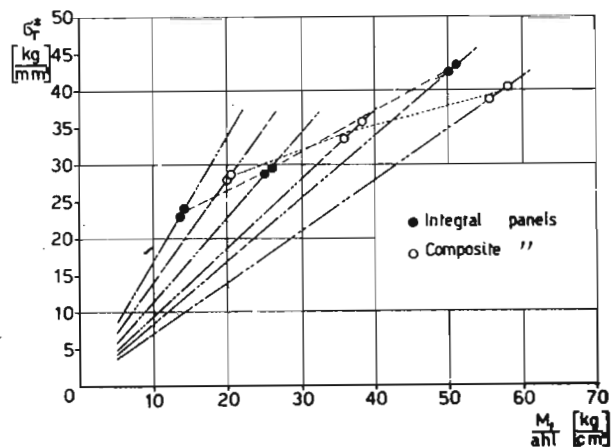
(*) Similar trends are reported by P.E.Sandorf (5).

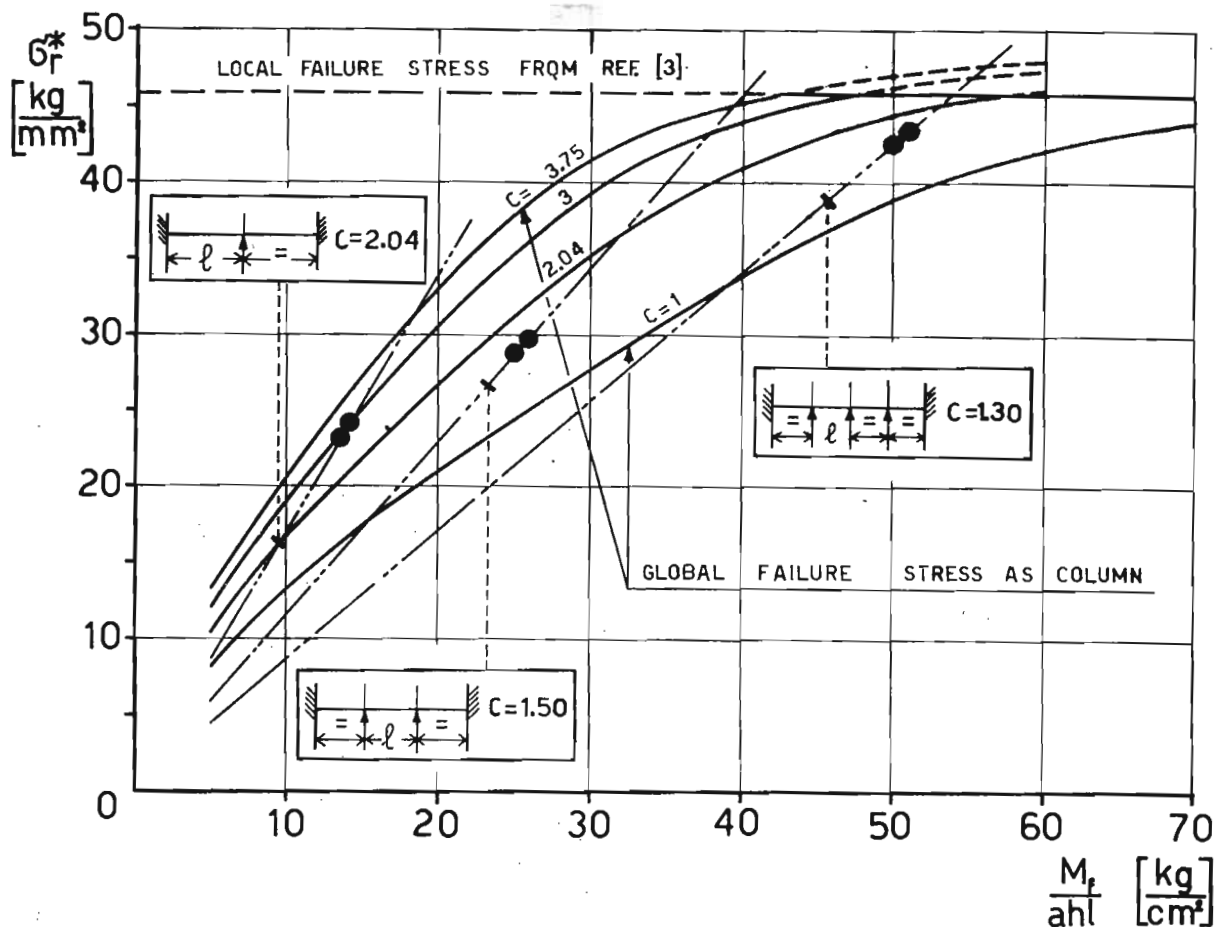FIG.18 – Failure experimental results (summary).

11

FIG. 19 – Comparison between experimental results and data of compressed panels with free lateral edges.
a) Integral panel specimens.

question should be 15% and 16%, for the integral panel and the composite panel respectively. Apparently in non – destructive tests, deviation values were obtained which a range from 85% to negative values above 200%. These values are significant for the typical structures of box wings. They should be kept into account when considering the effects of phenomena connected with the appearance of local bucklings, increase of local stresses, etc. From trends of $\Delta \sigma / \sigma_m$ in terms of M/ahl (Fig.17), one can clearly locate the load levels where appear divergent deformations, which are typical of instability phenomena.

Conclusions

The experimental results evidentiate that in wing boxes subject to bending, panels (particularly the compressed ones) show remarkable deformations in a direction normal to their barycentric surface. Such deformations affect both local values of stresses and collapsing local value of structures, and originate from deformations induced in panels as integral parts of boxes, as well

as from the presence of initial imperfections in the structure. They are affected by the actual boundary conditions of panels in the structure.

In particular, because of the above induced effects, anticlastic curvature of wing box, with flexural deformation of bulkheads and crushing pressure, also exert their influence, as one can see from test results. In addition to deformations due to such causes, phenomena of local instability may manifest as well.

With increasing loads, all the deformations follow trends revealing the presence of divergent components that cause the attainment of critical local stresses.
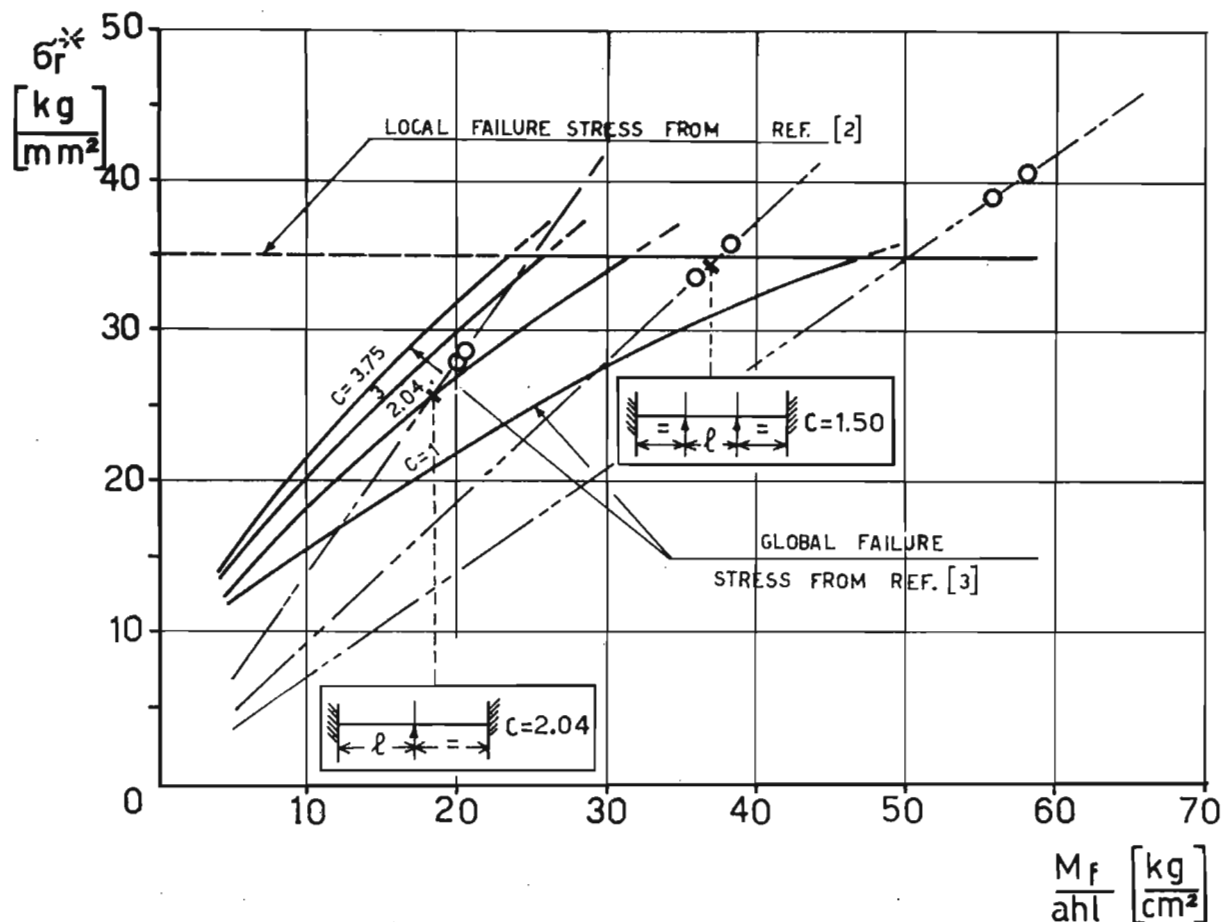
FIG. 19 – Comparison between experimental results and data of compressed panels with free lateral edges.
b) Composite panel specimens.

R E F E R E N C E S

(1) E.E.LUNDQUIST : Comparison of three methods for calculating the compressive strength of flat and slightly curved sheet and stiffener combinations.
NACA TN.455, 1933.

(2) H.B.CROCKETT : Predicting stiffener and stiffened panel crippling stresses.
J.A.S., 11/1942.

(3) SHUETTE : Observations on the maximum average stress of flat plates buckled in edge compression.
NACA TN.1157, February 1949.

(4) J.H.ARGYRIS : A study on instability and failure of stiffened panels under compression when buckling in long wavelengths.
Aircraft Engineering, June 1954.

(5) P.E.SANDORF : Design of structural models, with application to stiffened panels under combined shear and compression.
J.A.S., July 1956.

(6) P.KÜHN : Stresses in aircraft and shell structures.
Ed.Mc Graw – Hill Book Co., Inc., 1956

(7) G.GABRIELLI : Lezioni sulla scienza del progetto degli aeromobili. Vol. I
Libreria Editrice Universitaria Levrotto & Bella, Torino 1961.

(8) G.GERARD : Compressive strength of flat stiffened panels.
NACA TN. 3785, 1957.

(9) E.ANTONA : Effetto della pressione ortogonale e fenomeni di instabilità globale nei pannelli compressi dei cassoni alari soggetti a flessione.
Istituto di Progetto di Aeromobili del Politecnico di Torino, dicembre 1967.

(10) E.ANTONA – P.PELAGALLI : Analisi strutturale dei cassoni alari bilongheroni soggetti a flessione in campo elastico.
Atti e Rassegna Tecnica della Società degli Ingegneri e Architetti in Torino, dicembre 1968.

(11) P.CICALA   : Scienza delle costruzioni.
     Parte I^.
     Libreria Editrice Universitaria Levrotto &
     Bella, Torino 1968.

(12) G.GABRIELLI-P.M.MASSA-V.SACCHI : Rassegna
     dei risultati di prove di compressione su
     pannelli piani irrigiditi longitudinalmente
     e loro utilizzazione per il progetto di strut
     ture di minimo peso.
     Ingegneria, n° 1, gennaio 1970.

ICAS PAPER N°70-33

Page	Column	Line	Error	Correction
2	I	26	Staring	Starting
2	I	29	cecrease	decrease
2	I	32	values than	values lower than
2	II	6	pane	panel
2	II	29	turning	running
3	II	11	...of 1 350...	...of 1 are 350...
3	II	Fig.3	stiffened	⌐ - stiffened
4	I	9	spars	spans
4	II	4	as to as to	as to
4	II	6	at load	at lower load
			loads	load
5	II	17	compresssed	compressed
5	II	11	spans	span
5	II	31	a failure	at failure